A Multiple-Feed Connected Leaky Slot Antenna for In-Antenna Power Combining in 0.13 μm SiGe BiCMOS Technology

Jiangcheng Chen, Shihai He, Markus Berg, Aarno Pärssinen,
Centre for Wireless Communications - Radio Technologies Research Unit (CWC-RT), University of Oulu, Finland,
jiangcheng.chen@oulu.fi

***Abstract*—In this paper, a differentially-driven wideband multiple-feed on-chip antenna design in 0.13 μm SiGe technology is proposed for millimeter-wave power combining applications. The in-antenna power combining concept is achieved by combining parallel amplifiers in the multi-port radiator where each port corresponds directly to a differential power amplifier (PA) stage. Specifically, the radiator is composed of a leaky slot with multiple set of differential microstrip feed lines. A wideband Marchand balun with 1.5 dB insertion loss is applied to convert the differential output to the single-ended input of microstrip feed line. In addition, the proposed differential PA has a combined output power of 10 dBm and its output is directly connected with the balun. As a result, the proposed multiple-feed antenna has four differential microstrip feed lines connected with four Marchand baluns which are driven by four parallel differential PAs respectively. Also, to compensate for the loss along the signal route such as power splitters and baluns, pre-amplification PA stage is a necessity at the input of each PA stage. In order to suppress the surface waves in the high permittivity substrate, an extended hemispherical silicon lens is integrated with the chip. Simulation results show that the antenna can cover more than 50 % fractional bandwidth at 250 GHz and calculated EIRP is 19.3 dBm.**

***Index Terms*—on-chip antenna, connected slot antenna, power combining, multiple-port antenna, SiGe BiCOMS.**

I. Introduction

In these days, as ever-increasing demand on the required operational bandwidth due to the limited throughput of wireless link with current 5G mm-Wave frequency bands [1], sub-terahertz (sub-THz) and THz frequency bands are getting increasingly more focus and promising for future THz wireless systems with more than 100 Gbps or even one Tbps achievable date rate [2] [3]. Antenna implementation on traditional mm-Wave domain allows the use of System-on-package (SoP) solutions in which the the antenna elements are achieved by using low-loss microwave substrates and connected to RFIC modules through a certain feeding network and interconnects e.g. flip-chip or wire bonds, with acceptable loss level [4]. However, in these new spectrums namely sub-THz or THz frequencies, the off-chip SoP solution will suffer from considerable routing losses in passive components and interconnects due to the increased metal losses [5]. In this case, the system-on-chip (SoC) solution is a more preferred option that integrates the antenna element on the same chip with the RF front-end circuits e.g. power amplifier [6] [7] or tripler [8].

On the other hand, in addition to the large loss on the passive components, the output power of a amplifier stage is limited in high frequency range because of the physical nature of gate lengths or emitter areas which confine the current consumption and breakdown voltage of transistor devices [6]. The power combining, therefore, is of necessity and benefit. In general, this can be achieved by three approaches that are: (1) traditionally a power combiner, such as Wilkinson and transformer, that combines a certain number of PAs to the antenna input, (2) quasi-optical or free space power combining based on antenna array in which each antenna element is associated with an individual PA element in one RF chain [9] [10], and (3) multi-port antenna by which it enables the power-combining in the antenna element itself using multi-feed structure and each port connects to the nearby PA stage by eliminating long feed lines and lossy passive components [6] [11] [12] [13]. In (1), the solution is not promising due to the increased insertion loss of passive components as the number of amplifier increases and the passive loss is even higher than gain improved by parallel amplifiers. The quasi-optical or free space power combining in (2) results in a large chip area and the required long feed lines, in turn, lead to further loss. As for (3), it eliminates the long and large passive power combining network including both the passive components like couplers, splitters, and combiners as well as the transmission lines. Meanwhile, the chip with multi-port radiator remains compact size when amplifier elements are connected, which makes it cost-effective and favorable candidate for power combining.

The array of connected leaky-wave slots has proven to be capable of large relative bandwidth and high-efficiency illumination of the extended hemispherical lens [14]. Moreover, the inter element spacing of the feed of the leaky-wave slot can be electrically close ($0.08\lambda_0$), indicating its potential on multi-port operation [15] with appropriate feeding structure reported in [6], [12] and [13]. In this paper, a differentially-driven multi-port connected leaky-wave slot antenna in 0.13 μm SiGe Technology is presented. The full-wave simulations are conducted in CST Microwave Studio co-designed with Design Studio as well as ADS Momentum. To avoid the excitation of substrate modes, a silicon hemispherical lens which has similar dielectric constant as the Si substrate (ε_r=11.9) is applied and integrated with a silicon extended hemispherical lens [16]. Also, the silicon lens is used partially

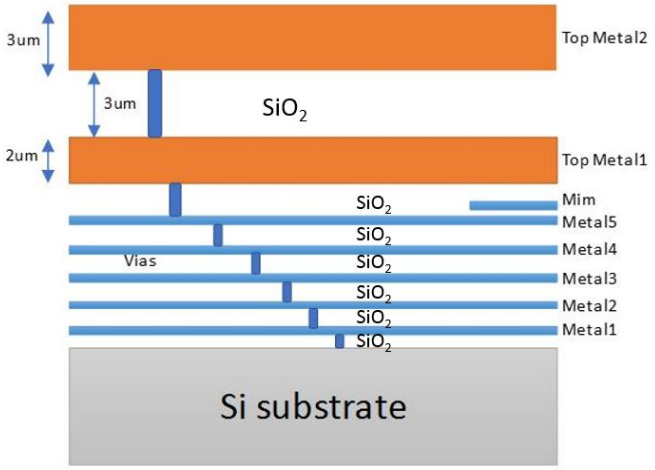

Fig. 1. 130 nm SiGe BEOL process cross-section

as a heat sink [17]. The multi-port radiator, which combines four differential power amplifiers as one example, is placed at the focal plane of the lens. In addition, a broadband Marchand balun is designed for purpose of combining the output power from the differential PAs. Consequently, a differential feeding configuration is implemented to drive the leaky slot with the capability of power combining.

II. ANTENNA DESIGN

The on-chip antenna is designed based on the SiGe back end of line (BEOL) process as shown in Fig. 1. This technology provides seven metal layers including two thick low loss metal layers for signal transmission and five thin metal layers for connections. The on-chip antenna contains a thick Si (ε_r=11.9) substrate and a thin SiO_2 (ε_r=4.1) with a thickness of 200 μm and 15 μm. Fig. 2a shows the perspective view of the on-chip antenna placed on the focal plane of the silicon hemispherical lens which has a diameter of 4 mm and extension height of 635 μm. The thickness of silicon substrate and extension height of the hemispherical lens are chosen to ensure the antenna element locate on the focal plane. Besides, the silicon substrate is directly placed on the surface of the lens without any gap. The radiation from the leaky slot, thus, is directed to the backside of the chip through the substrate and lens. Different from [14] which leaky-wave slot is fed by individual elements, the proposed antenna with eight-feed shown in Fig. 2b adopts two parallel dual closely placed microstrip lines as feed element. Based on the four-feed concept in [13], the design is extended to eight-feed configuration by using electrically close microstrip lines with a spacing of 10 μm which is determined by the signal to ground distance to lower the coupling. The microstrip lines are located in layer Top Metal 2 while the ground plane with the leaky slot is in layer Metal 1. Each feed line is excited differentially with out of phase signal at each end (input) of the line and with signal

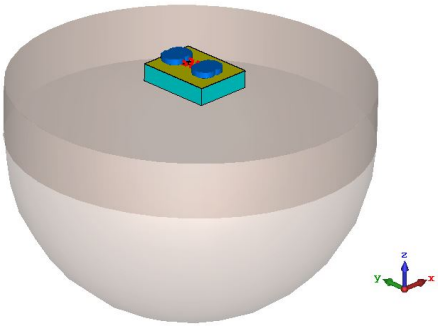

(a)

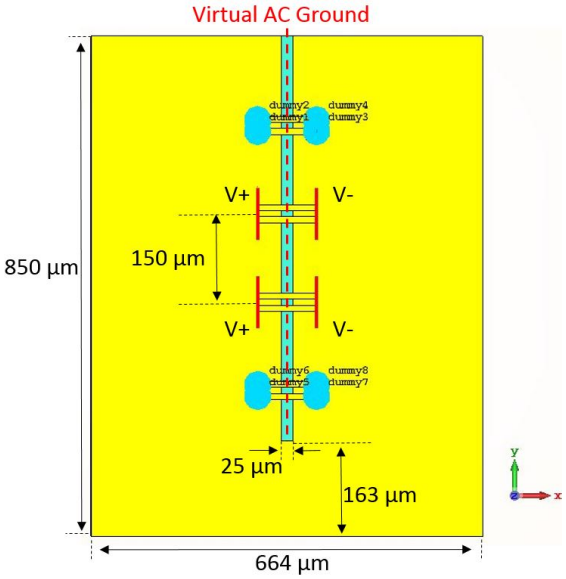

(b)

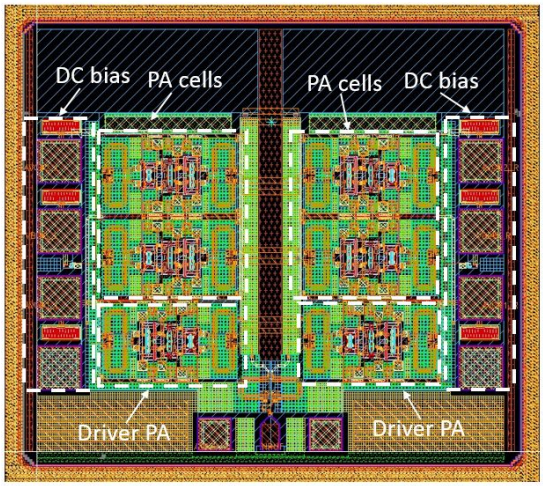

(c)

Fig. 2. The configuration of the proposed multi-port on-chip antenna: (a) perspective view with integrated hemispherical silicon lens, (b) eight-feed on-chip antenna, and (c) layout of the multi-port radiator incorporating amplifier stages and differential feeding network in Cadence.

in phase at left and right columns respectively. Consequently,

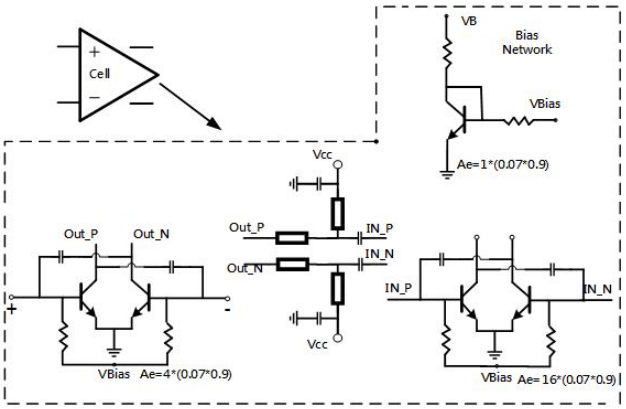

Fig. 3. Schematic of the two-stage amplifier unit

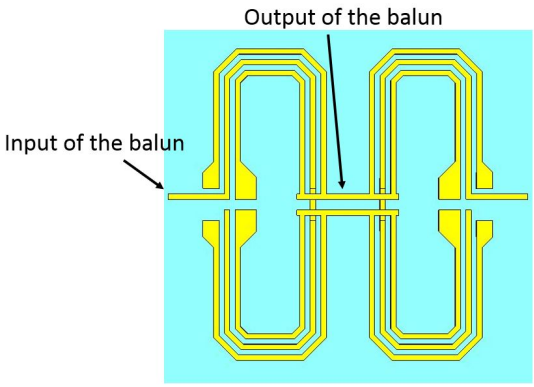

Fig. 4. Top view of the back-to-back Marchand balun structure

the excitations for all microstrip lines are in phase so that the coupling between closely-placed feed lines is negligible [6]. The feed technique of differential microstrip transmission line for the leaky slot is similar as that in [18]. Furthermore, compared to the differential drive of a slot radiator in [13] which uses two separate microstrip lines crossing over the slot and shorted at opposite sides of the slot with out of phase signals, our work applies one microstrip line over the slot, which is excited by two feeds at two ends with same amplitude and opposite phase, leading to the a virtual short circuit in the middle of the feed lines. The currents on the same line from opposite feeds at the ends, in turn, add up constructively without increasing the voltage at the input ports. This current superposition thereby enables high currents for high power design as well as low output impedance design of the power amplifier stage to overcome the limited peak voltage of the transistors [5]. The real and imaginary part of input impedance of the multi-port antenna is tuned by modifying the width of microstrip feed lines and width of the leaky slot, which is designed to match the output impedance of the PA.

As can be also seen Fig. 2b, two dummy elements are added beside the feeding elements separately to behave the mutual coupling effect of ohmic dissipation into the edge or neighboring elements [14] and thus overcome the edge element effect. To be more precise, the operating antenna element, fed by four microstrip lines and eight ports, is the leaky slot part as one unit cell where in between two dummy elements with a total length of around 300 μm. The slot length, ground size and number of input ports are a tradeoff between the size of chip and maximum integrated number of amplifier stage (depending on the area of each amplifier unit). Although tens of ports are implemented in [15], the massively coherent feed is not feasible because the spacing is too small to accommodate for one amplifier and other circuits. On top of that, the slot is not extended for further feed elements as the radiation from the leaky slot will lose the Gaussicity and hence degrade the gain of the lens and broaden or tilt the beam with off-axis active elements in the focal plane. Therefore, from above discussions, four differential power amplifiers are employed for eight-feed antenna as a compromise in this work,.

It is also noted that the leaky slot which is terminated by an open end on one side and a shorted end on the other side in 2b differs from those in [14] and [15] with both open ends. This results from the fact that the short-circuit side is used to accommodate for the input circuit and the ground should be kept complete for the components (e.g. GSG pads and Marchand balun in our case), In this way, the whole layout remains symmetric for the ease of signal routing and the differential signals come out of the input stage (the Marchand balun) keeps balanced when they are transferred with same route length to the input ports of the microstrip lines in the left and right columns respectively.

The whole layout of the proposed multi-port radiator including power splitting network and amplifier stages is shown in Fig. 2c. It can be seen that there is a guard ring enclosing the ground layout required by the process. The pads on the left and right sides are DC bias for the active PA elements. In addition, pre-amplification stages (driver PAs) are needed to compensate for the large path loss from the output of the Marchand balun to the input of PA stages. The output of the driver state splits into two ways and each branch is connected to a PA cell that feeds two closely placed inputs of microstrip line. In between the PA and feed line, there exists a Marchand balun to covert the different output of PA to single-ended feedline and a small two-way power splitter is needed to connect from the single-ended output of balun to two closely placed microstrip inputs. It is worthy to mention that the 80-μm-wide DC bias added on the left and right edges increase the total width of layout.

III. Power amplifier and Balun Design

This PA is implemented in IHP's 130 nm SiGe BiCMOS technology SG13G2 with f_t/f_{max} of 300/500 GHz. As shown in Fig. 3, each PA unit includes a two-stage common emitter differential amplifier and it is designated to operate at frequency band of 230–290 GHz. Since the high loss of the zero-degree power splitter at high frequency, the emitter area of first stage is a quarter of the second stage. For high output power, large device is necessary. However, the output impedance decreases greatly with the size, which will be sensitive for the output matching network. The number

of emitter fingers in this process can be varied from 1 to 10. Considering the tradeoff between high output power and output matching, the size of second stage is optimized to 32 $\times$ (0.07 $\times$ 0.9 μm^2) where 32 is the number of transistors. This amplifier unit shows an output impedance of 40+j*0 Ω (for each single-ended port of the differential output) with which the input impedance of the antenna feed line are designed. A Marchand balun introduced in [19] is applied at the the RF input to generate wideband differential signal for mircrostrip feed lines of the leaky slot and the back-to-back structure is represented in Fig. 4. The input of balun is single-ended while the output is differential.

IV. Simulation Results

In the simulation, four waveguide ports set as multipin ports are used for each end of microstrip line and combined differentially with ideal 3-dB power dividers in CST DS to obtain the input reflection coefficient of the multi-port antenna. As can be seen in Fig. 5, the antenna is well-matched to the differential power amplifier output impedance of 80 Ω and it show a broadband 10-dB matching with over 50 $\%$ relative bandwidth covering the designated operation band at 250 GHz. The radiation pattern in both E- and H-plane at the operation frequency are also shown in Fig.6, indicating a broadside realized gain of 16.9 dBi at 250 GHz with the lens of 4-mm diameter and 635-μm extension height. Also, as noted the E-plane pattern has higher side lobe level than that of H-plane due to fact that the E- and H-plane illumination from the near field source (the leaky slot) have different distance from the location of focal point, which is also referred as astigmatism from optics perspective [20]. This results in correct plane wave (the secondary radiation from lens) in H-plane while it leads to de-focused fields in E-plane such that the side lobe level rises. Moreover, although most power radiated from leaky slot is coupled to the silicon lens [16], the back radiation still exists because of absence of back reflector structure.

The simulated insertion loss of one broadband Marchand balun is around 1.5 dB at 250 GHz as illustrated in Fig.7. The gain of the amplifier is depicted in Fig.8 that with matching at the input impedance of 50 Ω as well as output impedance of 40 Ω (at each differential-ended port) the peak gain of 5.8 dB over operation frequency is observed. Moreover, each PA cell consumes 80 mA and all take 240 mA current from a 2 V supply voltage, leading to a DC power of 480 mW. Simulated in ADS Momentum, the proposed power amplifier (6 PA cells) has a maximum combined output power of 10 dBm in the frequency range of 230–260 GHz and the gain gradually decreases as frequency goes to higher due to the physical feature of the transistors. The two-way power splitter between the output of balun and input of two closely placed microstrip lines shows a loss of 0.4 dB. Considering the gain of antenna of 16.9 dBi and path loss at four baluns and four power splitters, the multi-port radiator including power amplifier gives rise to a simulated EIRP of 19.3 dBm.

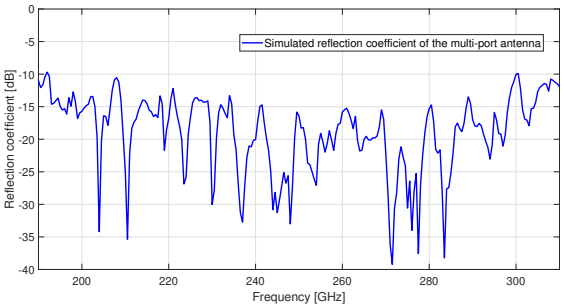

Fig. 5. The simulated active reflection coefficient of the multi-port antenna combined by an ideal balanced port with a differential impedance of 80+j*0 Ω and 3-dB power dividers

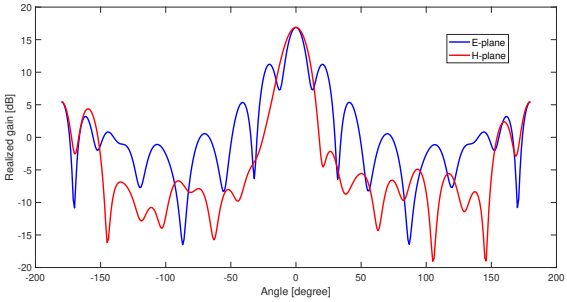

Fig. 6. The simulated realized gain pattern in both E- and H-plane at 250 GHz of the proposed eight-feed differential leaky slot antenna integrated with a hemispheric silicon lens with a diameter of 4 mm.

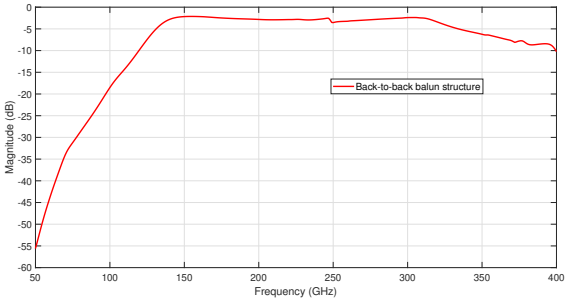

Fig. 7. Simulated insertion loss of back-to-back Marchand balun structure.

Comparison of the proposed multi-feed antenna with reported works is given in Table I.

V. Conclusion

In this paper, a differentially driven leaky slot on-chip antenna based on 0.13 μm SiGe Technology is proposed for in-antenna power combining. Fed by four microstrip lines with differential excitation, the leaky slot antenna achieves eight ports driven by four parallel PA cells in a compact area. Simulation results show that with the assistant of silicon lens, the surface modes in the thick Si substrate is suppressed, in turn, the multi-feed antenna has a fractional bandwidth over 50%, and 16.9 dBi realized gain is obtained at 250 GHz

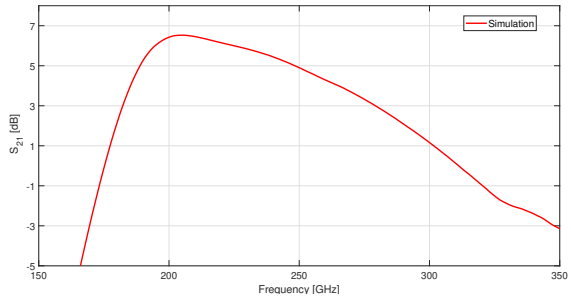

Fig. 8. The simulated gain of the power amplifier, which is calculated with 50 Ω input impedance and 40 Ω output impedance

TABLE I
COMPARISON OF MULTI-FEED ANTENNA IN SILICON WITH IN-ANTENNA POWER COMBINING ABOVE 150 GHZ

Design	[6]	[5]	This work
Frequency	240	161	250
Size [mm^2]	0.51	1	0.64
Process	130 nm SiGe	130 nm SiGe	130 nm SiGe
External Optics (lens)	Yes	None	Yes
DC Power [mW]	496	388	480
EIRP [dBm]	n/a	4.6	19.3 (simulated)

which is the center operation frequency of the amplifier stage. Moreover, with a maximum combined power of 10 dBm, the designed power amplifier can operate in 230–290 GHz. The calculated EIRP is 19.3 dBm taking into account the enhanced gain from lens and passive losses e.g. baluns and power splitters.

ACKNOWLEDGMENT

This work was supported in part by the Academy of Finland 6Genesis Flagship (grant no. 318927).

REFERENCES

[1] J. G. Andrews et al., "What Will 5G Be?," in IEEE Journal on Selected Areas in Communications, vol. 32, no. 6, pp. 1065-1082, June 2014.
[2] N. Sarmah et al., "A Fully Integrated 240-GHz Direct-Conversion Quadrature Transmitter and Receiver Chipset in SiGe Technology," in IEEE Transactions on Microwave Theory and Techniques, vol. 64, no. 2, pp. 562-574, Feb. 2016.
[3] J. Grzyb, P. R. Vazquez, N. Sarmah, W. Förster, B. Heinemann and U. Pfeiffer, "High data-rate communication link at 240 GHz with on-chip antenna-integrated transmitter and receiver modules in SiGe HBT technology," 2017 11th European Conference on Antennas and Propagation (EUCAP), Paris, 2017, pp. 1369-1373.
[4] W. T. Khan et al., "A D-Band Micromachined End-Fire Antenna in 130-nm SiGe BiCMOS Technology," in IEEE Transactions on Antennas and Propagation, vol. 63, no. 6, pp. 2449-2459, June 2015.
[5] S. M. Bowers and A. Hajimiri, "Multi-Port Driven Radiators," in IEEE Transactions on Microwave Theory and Techniques, vol. 61, no. 12, pp. 4428-4441, Dec. 2013.
[6] B. Goettel, P. Pahl, C. Kutschker, S. Malz, U. R. Pfeiffer and T. Zwick, "Active Multiple Feed On-Chip Antennas With Efficient In-Antenna Power Combining Operating at 200–320 GHz," in IEEE Transactions on Antennas and Propagation, vol. 65, no. 2, pp. 416-423, Feb. 2017.
[7] Z. Wang, P. Chiang, P. Nazari, C. Wang, Z. Chen and P. Heydari, "A CMOS 210-GHz Fundamental Transceiver With OOK Modulation," in IEEE Journal of Solid-State Circuits, vol. 49, no. 3, pp. 564-580, March 2014.
[8] S. Hu et al., "A SiGe BiCMOS Transmitter/Receiver Chipset With On-Chip SIW Antennas for Terahertz Applications," in IEEE Journal of Solid-State Circuits, vol. 47, no. 11, pp. 2654-2664, Nov. 2012.
[9] Y. A. Atesal, B. Cetinoneri, M. Chang, R. Alhalabi and G. M. Rebeiz, "Millimeter-Wave Wafer-Scale Silicon BiCMOS Power Amplifiers Using Free-Space Power Combining," in IEEE Transactions on Microwave Theory and Techniques, vol. 59, no. 4, pp. 954-965, April 2011.
[10] M. E. Bialkowski and H. J. Song, "Investigations into a power-combining structure using a reflectarray of dual-feed aperture-coupled microstrip patch antennas," in IEEE Transactions on Antennas and Propagation, vol. 50, no. 6, pp. 841-849, June 2002.
[11] B. Goettel, J. Schäfer, A. Bhutani, H. Gulan and T. Zwick, "In-antenna power-combining methods," 2017 11th European Conference on Antennas and Propagation (EUCAP), Paris, 2017, pp. 2776-2730.
[12] S. Li, T. Chi, Y. Wang and H. Wang, "A Millimeter-Wave Dual-Feed Square Loop Antenna for 5G Communications," in IEEE Transactions on Antennas and Propagation, vol. 65, no. 12, pp. 6317-6328, Dec. 2017.
[13] T. Chi, S. Li, J. S. Park and H. Wang, "A Multifeed Antenna for High-Efficiency On-Antenna Power Combining," in IEEE Transactions on Antennas and Propagation, vol. 65, no. 12, pp. 6937-6951, Dec. 2017.
[14] D. Cavallo and A. Neto, "A Connected Array of Slots Supporting Broadband Leaky Waves," in IEEE Transactions on Antennas and Propagation, vol. 61, no. 4, pp. 1986-1994, April 2013.
[15] O. Yurduseven, D. Cavallo and A. Neto, "Wideband Dielectric Lens Antenna With Stable Radiation Patterns Fed by Coherent Array of Connected Leaky Slots," in IEEE Transactions on Antennas and Propagation, vol. 62, no. 4, pp. 1895-1902, April 2014.
[16] D. F. Filipovic, S. S. Gearhart and G. M. Rebeiz, "Double-slot antennas on extended hemispherical and elliptical silicon dielectric lenses," in IEEE Transactions on Microwave Theory and Techniques, vol. 41, no. 10, pp. 1738-1749, Oct. 1993.
[17] J. Grzyb, K. Statnikov, N. Sarmah, B. Heinemann and U. R. Pfeiffer, "A 210–270-GHz Circularly Polarized FMCW Radar With a Single-Lens-Coupled SiGe HBT Chip," in IEEE Transactions on Terahertz Science and Technology, vol. 6, no. 6, pp. 771-783, Nov. 2016.
[18] O. Yurduseven, N. Llombart Juan and A. Neto, "A Dual-Polarized Leaky Lens Antenna for Wideband Focal Plane Arrays," in IEEE Transactions on Antennas and Propagation, vol. 64, no. 8, pp. 3330-3337, Aug. 2016.
[19] Ahmed, F., Furqan, M., Aufinger, K., Stelzer, A. (2017). Analysis and design of a high-gain 100–180-GHz differential power amplifier in 130 nm SiGe BiCMOS. International Journal of Microwave and Wireless Technologies, 9(6), 1231-1239.
[20] O. Quevedo-Teruel, M. Ebrahimpouri and F. Ghasemifard, "Lens Antennas for 5G Communications Systems," in IEEE Communications Magazine, vol. 56, no. 7, pp. 36-41, July 2018.